e-ISSN: 0975-1556, p-ISSN:2820-2643

Available online on www.ijpcr.com

International Journal of Pharmaceutical and Clinical Research 2024; 16(2); 1402-1410

Original Research Article

Magnetic Resonance Imaging in Evaluation of Musculoskeletal Tumors

Nath A[1*], Pegu BJ[2], Kutum T[3]

[1]Post Graduate Trainee, Department of Radiology, Silchar Medical College and Hospital, Assam
[2,3]Assistant Professor, Department of Radiology, Silchar Medical College and Hospital, Assam

Received: 25-11-2023 / Revised: 23-12-2023 / Accepted: 26-01-2024
Corresponding Author: Dr. Nath A
Conflict of interest: Nil

Abstract:

Bone tumors and tumor-like lesions are frequently encountered by radiologists. Although radiographs are the primary screening technique, magnetic resonance imaging (MRI) can help narrow the differential or make a specific diagnosis when a lesion is indeterminate or shows signs of aggressiveness. MRI can extend the diagnostic evaluation by demonstrating several tissue components. Even when a specific diagnosis cannot be made, the differential diagnosis can be narrowed. MRI is superior to the other imaging modalities in detecting bone marrow lesions and tumoral tissue (faint lytic/sclerotic bone lesions can be difficult to visualize using only radiographs). Contrast-enhanced MRI can reveal the most vascularized parts of the tumor and MRI guidance makes it possible to avoid biopsing necrotic areas. MRI is very helpful in local staging and surgical planning by assessing the degree of intramedullary extension and invasion of the adjacent physeal plates, joints, muscle compartments and neurovascular bundles. It can be used in assessing response to neoadjuvant therapy and further restaging. The post-therapeutic follow-up should also be done using MRI. Despite the high quality of MRI, there are a few pitfalls and limitations of which one should be aware. Applications of MRI in bone tumors will probably continue to grow as new sequences are further studied.

Keywords: Magnetic resonance imaging, Bone neoplasms, Diagnosis, Neoplasm staging, Follow-up.

Introduction

The term bone tumor is a broad category, encompassing benign and malignant neoplasms, reactive focal abnormalities, metabolic abnormalities, and miscellaneous "tumorlike" conditions. The location of the tumor and the patient's age are the two most crucial factors in evaluating a bone tumor. Without even examining any photos, this information alone can be used to restrict the differential diagnosis. The particular radiographic appearance will therefore frequently result in the single accurate diagnosis and aid further reduces the list.

The method for radiographic diagnosis of bone tumors involves systematically examining the lesion and taking note of various distinct radiographic characteristics [1–5]. Although these characteristics were first explained in relation to how the lesion appeared on traditional radiographs, computed tomographic (CT) scans can also be used to apply them [6].

Nevertheless, they are inapplicable to magnetic resonance (MR) images, since marrow and soft-tissue edema can overstate the severity of certain benign lesions on MR images [7–9]. Tumor location, borders and zone of transition, periosteal reaction, mineralization, size and number of lesions, and presence of a soft-tissue component are the specific radiographic findings that need to be assessed.

Case Series

Case 1- Unicameral bone cyst/ Simple bone cyst (SBC): Unicameral bone cysts account for 3% of benign bone tumors [10]. The most frequent consequences are recurrent pathologic fractures and bone growth abnormalities because the site is frequently metaphyseal and adjacent to the physics; spontaneous healing happens in 5%–10% of instances [11–13]. Reducing the chance of a pathologic fracture and accelerating osseous healing are the main objectives of percutaneous treatment for unicameral bone cysts. Unicameral bone cysts have been managed by a number of percutaneous procedures, such as intralesional steroid injection, autologous bone marrow concentrate, bone allograft, and demineralized bone matrix [14–16].

The most helpful modality for examining the internal structure of the lesions is magnetic resonance imaging (MRI), thanks to its excellent soft tissue contrast and multiplanar views. When a cyst is real, only its epithelial covering shows up

well on MRI; contrast-enhanced MRI shows no enhancement at all in the interior of the cyst [17]. Due to its non-epithelial lining, SBC may be distinguished from actual cysts with epithelial linings using contrast-enhanced MRI. Generally speaking, benign tumors—which need to be differentiated from SBCs—have solid contents, whereas SBCs are typically filled with fluid. Therefore, by examining the signal intensity (SI) on MRI, SBCs can be identified apart from benign tumors.

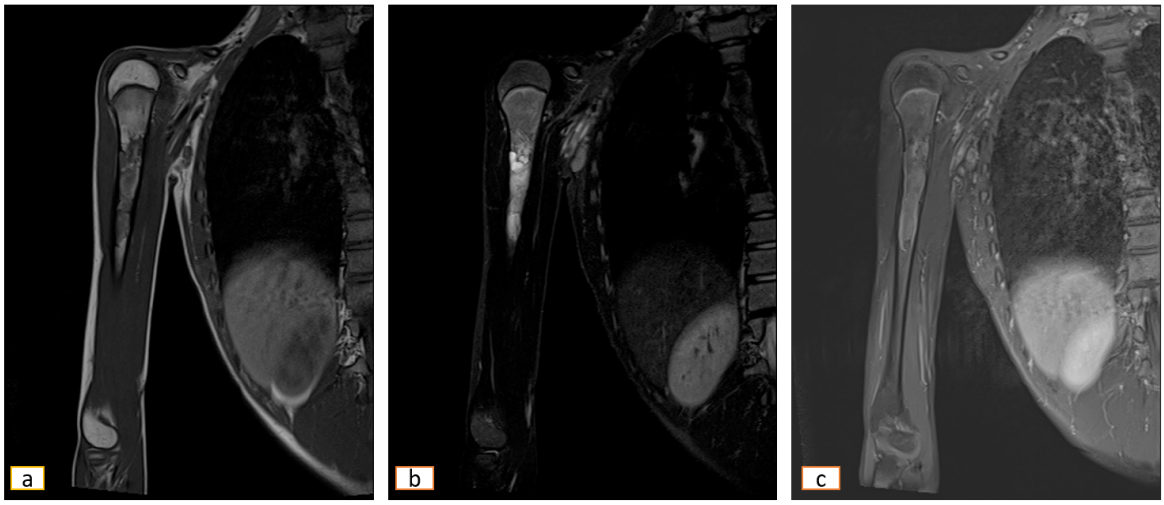

Figure 1: This humeral lesion in a 17 yr boy is showing a) low signal intensity in T1WI b) high signal in T2FS WI. c) T1FS gadolinium-based contrast medium-enhanced sequence showed peripheral enhancement, typical of liquid content, favouring the diagnosis of a solitary bone cyst.

Case 2- Aneurysmal bone cyst (ABC): Primary aneurysmal bone cysts are benign neoplasms that in 75% of cases affect patients younger than 20 years of age [10], The metaphysis of the long bone, the spine (usually the posterior components), and the pelvis are the common sites of primary aneurysmal bone cysts [10].

Due to the highly vascular nature of the tissue and sometimes difficult anatomic locations, surgical resection can be difficult to accomplish total excision, control of bleeding, weakening and instability of the bone, and damage to surrounding structures. There is also a significant risk of recurrence [12]. Magnetic resonance imaging demonstrates fluid-fluid levels. Low T1 and T2 signal rims can be seen on T1contrast-enhanced and T2 weighted images, which highlight the septa within the lesion [18]. Multiple focal areas of hyperintense signal on T1 and T2 weighted sequences indicate the presence of variable age blood within the cystic cavities; double density fluid levels may also be observed. Osseous and soft tissue edema may indicate the presence of a pathologic fracture.

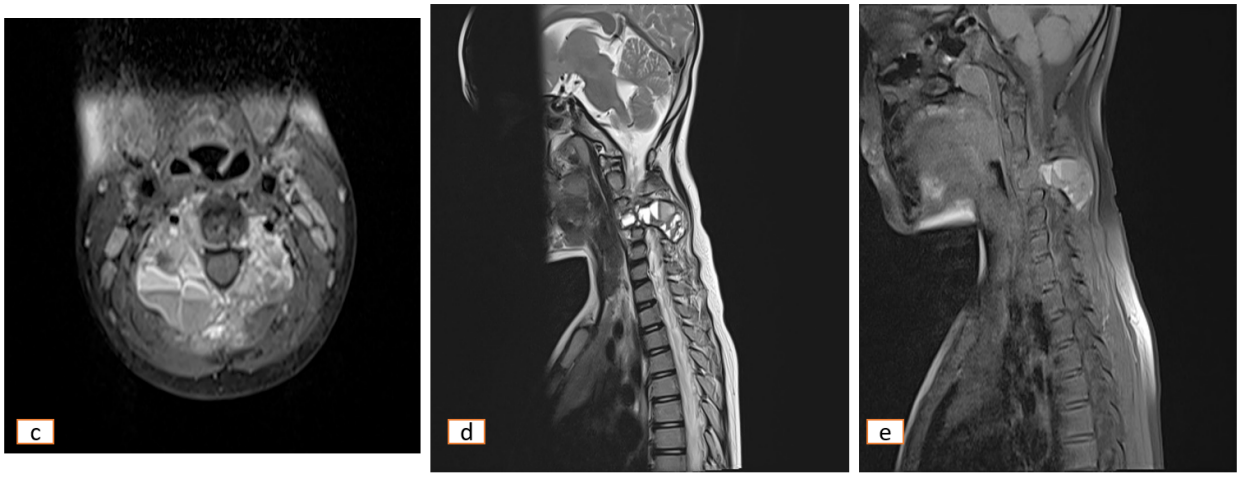

Figure 2: Expansile multiloculated cystic lytic lesion is seen involving C4 vertebra which is replacing whole of the body, lamina, pedicle, transverse process and spinal process causing moderate spinal canal stenosis and spinal cord indentation posteriorly. The lesion shows multiple internal fluid- fluid levels on c)

axial STIR, d) sagittal T2WI and e) STIR sequences, with no intervening soft tissue or thick septations, suggesting aneurysmal bone cyst.

Case 3- Fibrous dysplasia (FD): The distribution of FD lesions depends on the form of the disease. Monostotic FD accounts for about 80% of patients with FD. The most common location of monostotic FD is the rib, skull and femur. In the polyostotic form, the skull, mandible, pelvic bones and femur are the most frequently affected sites. While the majority of bony lesions in polyostotic FD become non-silent and clinically significant by the age of 10, virtually no new lesions appear after the age of 15. Many cases of monostotic FD are discovered incidentally, whereas the polyostotic form is typically diagnosed during the first few years of life. FD does not consistently show hypointense signal intensities on T1- and T2-weighted images (WI) as might be expected (19). Signal intensity on T1- and T2-WI and the degree of contrast enhancement depend on the amount and degree of bony trabeculae, cellularity, collagen, and cystic and hemorrhagic changes. Sharply defined borders and intermediate to low signal intensity on T1-WI and intermediate to high intensity on T2-WI are typical features of FD lesions. The T2 signal decreases with increasing bony trabeculae count and increases with decreasing bony trabeculae count.

Additionally, tiny cystic regions that brighten the T2 signal can be found in FD lesions. On postcontrast T1-WI, all lesions exhibited some degree of enhancement. Whereas inactive lesions exhibit a milder enhancement, active lesions exhibit an avid enhancement (20). The enhancement pattern could be homogeneous, rim, patchy in the center, or a combination of these.

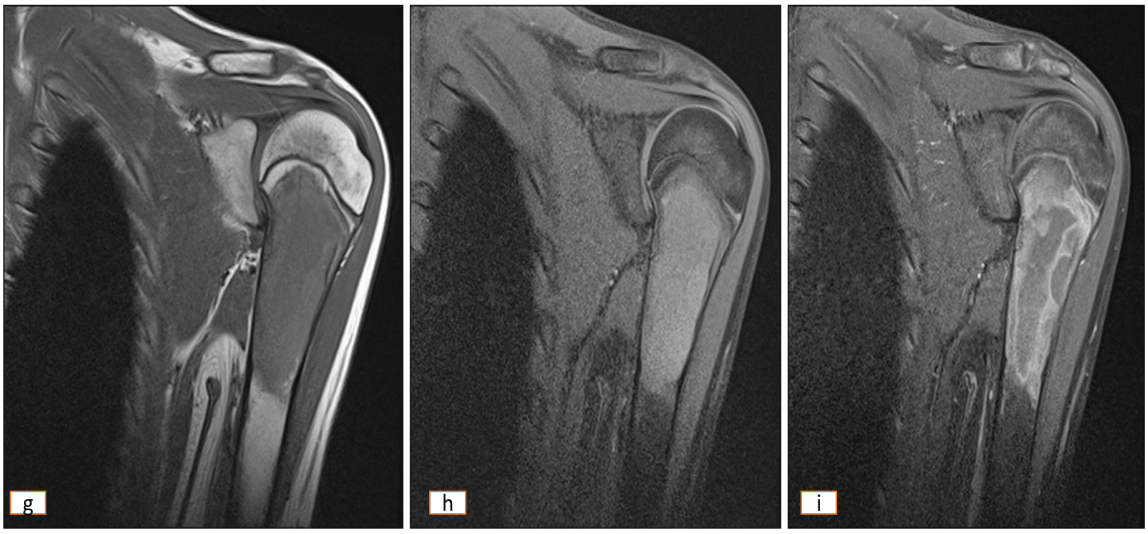

Figure 3- A multiloculated intramedullary g) T1 hypointense and h) STIR hyperintense lesion is noted in the proximal metaphysis and upper 1/3rd of diaphysis of left humerus showing i) peripheral enhancement on post contrast study. STIR hyperintensity is noted in the proximal epiphysis of the left humerus, suggesting edema.

Case 4- Ewing's sarcoma: Ewing's sarcomas are common bone tumors in children [21]. EES is less common, more frequently observed in older adults and children, and frequently has a worse prognosis [22,23]. Similar to its intraosseous counterpart, extraosseous Ewing's sarcoma (EES), which was initially reported in 1969, is a malignant mesenchymal tumor. These tumors are typically found in the deep soft tissues of the extremities or in the paravertebral regions; the lower extremities are more likely than the upper extremities to develop these tumors [21]. Individuals diagnosed with EES frequently report a rapidly expanding soft-tissue mass, of which approximately one-third is painful due to nearby structures being compressed. In the second decade of life, they frequently manifest. There is a slight preference for Caucasians and a male predominance.

No evidence of environmental or familial influence has been found [24–27].A mass with signal intensity comparable to skeletal muscle on T1-weighted imaging has been observed on magnetic resonance imaging (MRI) (21, 28); internal hemorrhage areas may be observed as high T1 signal [21,28. The mass frequently shows a heterogeneous intermediate to hyperintense signal on T2-weighted images. High T2 signal regions are frequently found at the sites of cystic or necrotic alterations. In postcontrast images, heterogeneous enhancement is frequently seen. It is also possible to observe high-flow vascular channels or flow

voids, which are very typical but not specific to EES.

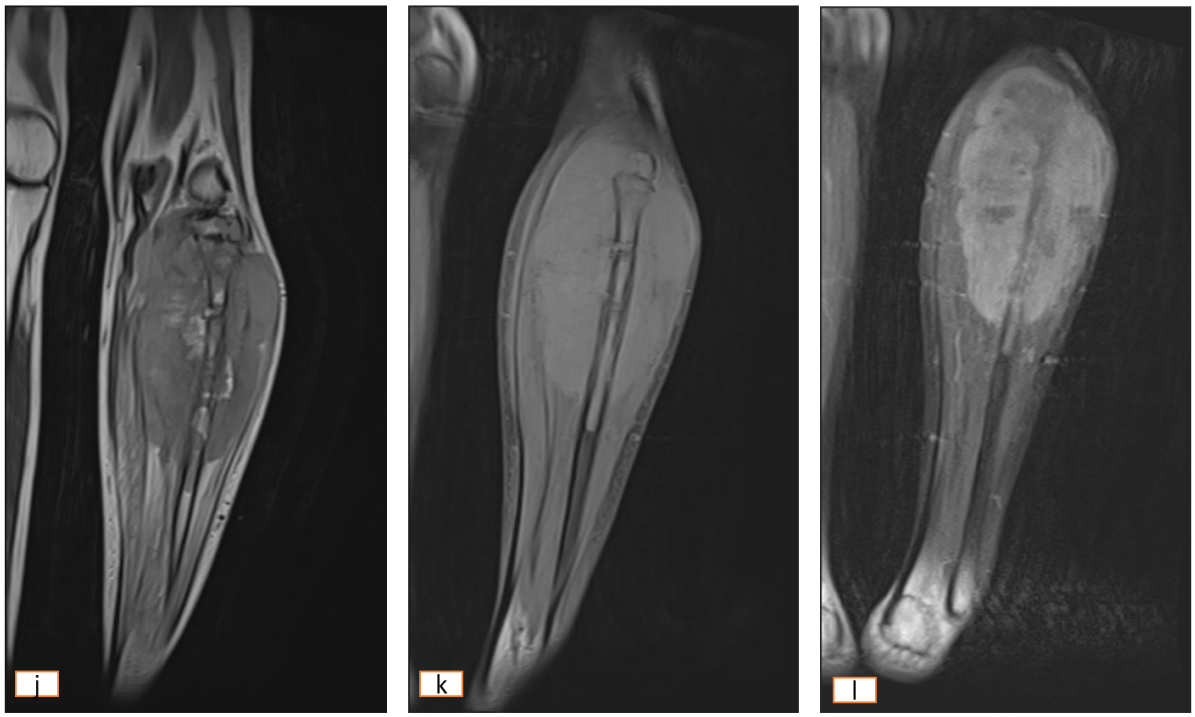

Figure 4: An expansile bone lesion centered in the upper half of left fibula with a soft tissue component, showing j) heterogenous signal intensity on T1WI, k) isointense on T2WI and l) heterogenous enhancement on post contrast study. Surrounding muscles appears edematous. Tumor shows extension into the posterolateral epiphysis of ipsilateral tibia. T1WI also shows lamellated periosteal reaction, suggesting it to be Ewing's sarcoma.

Case 5- Osteosarcoma: Osteosarcoma (OS) is a malignant tumor of connective tissue that produces osteoid matrix and variable amounts of cartilage matrix and fibrous tissue [29]. OS is the most common primary bone tumor in children and adolescents (4.4 cases per million persons per year), although it makes up less than 1% of all cancers diagnosed in the United States (30-32). Seven unique primary subtypes of osteosarcoma are recognized in the World Health Organization classification system: high-grade surface osteosarcomas, parosteal, periosteal, small cell, conventional, and telangiectatic osteosarcomas [33]. The most prevalent subtype of osteosarcoma, known as conventional or classic osteosarcoma, accounts for 75–80% of all cases [34,35]. Elevated surface subtypes, uncommon in kids [33,34]. A less common intramedullary subtype, telangiectatic osteosarcoma accounts for 2%–12% of cases [36-38] and can occasionally be misdiagnosed as an aneurysmal bone cyst [38]. In contrast to intramedullary osteosarcomas, which are confined within the medullary cavity, surface osteosarcomas "sit" on the surface of the bone. The rare childhood forms of surface osteosarcomas include parosteal, periosteal, and high-grade surface subtypes [33,34].

MRI is the preferred imaging modality for characterizing tumor bulk and extent of local invasion. Due to the intrinsic fatty elements of bone marrow, intramedullary tumors are best visualized on T1-weighted MR images where they appear as a low signal intensity area against a background of otherwise higher signal intensity [38–41]. On fluid-sensitive (T2-weighted fat-suppressed or short-tau inversion-recovery) MR images, the extent of the intramedullary tumor is overestimated in as many as 73% of cases [41, 42]. To describe tumor heterogeneity and show regions of cystic degeneration and necrosis, postcontrast T1-weighted MR images can be utilized.

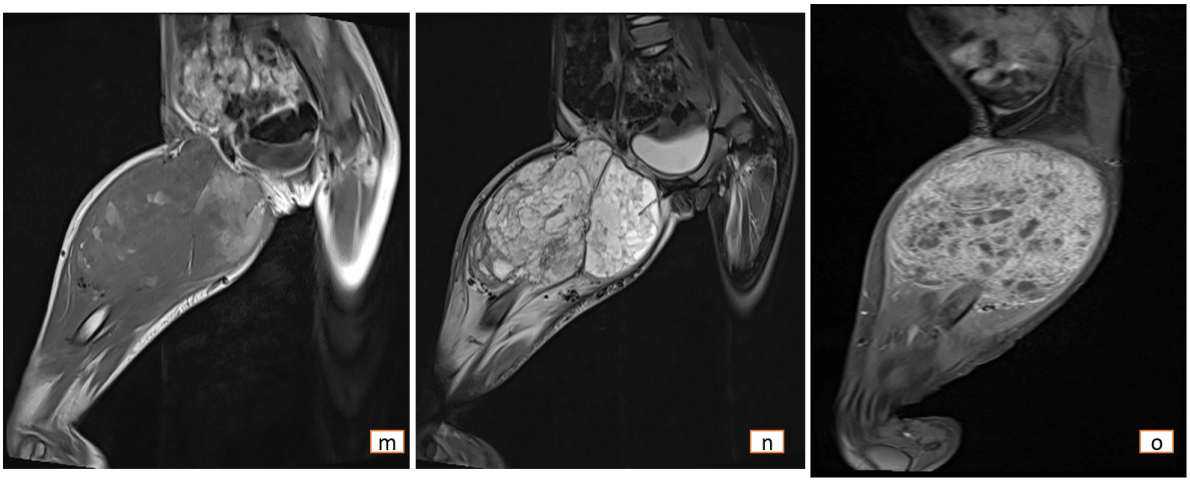

Figure 5: A large ill-defined lesion is noted involving the right femoral diaphysis with extension into the medullary cavity and epi-metaphyseal region limited by the physeal plate, with large soft tissue component which appears m) T1 isointense with areas of hyperintensity (suggesting Haemorrhagic foci) and n) T2 heterogeneously hyperintense intermixed with intermixed areas of hypointensity (suggesting osteoid matrix). o) T1FS gadolinium-based contrast medium-enhanced sequence showed heterogeneously enhancement. Soft tissue component invasion is noted into the muscles of anterior, middle and posterior component of upper and mid-thigh which is extending caudally till midshaft of femur and extending cranially till the ischiopubic rami. Features suggesting Osteosarcoma.

Case 6- Metastasis: Bone metastasis is frequently observed in the most relevant types of solid tumors representing an important imaging target for detection and follow-up. For this purpose, morphologic aspects of skeletal lesions are assessed by conventional X-rays, CT, and MRI, whereas bone scintigraphy and SPECT reveal changes of bone remodeling.

Most relevant types of solid tumors frequently show evidence of bone metastasis. Of these, skeletal metastatic lesions are present in about 70% of breast and prostate cancer patients who pass away from their illness. As a result, one of the most frequent locations for cancer to spread is to the skeleton. As a result, patients with skeletal complications like pathologic fractures, spinal cord compression, and hypercalcemia have much lower quality of life. Compared to other imaging modalities, magnetic resonance imaging (MRI) is particularly sensitive and specific in detecting bone metastases because of its superior soft-tissue contrast. Since tumor growth frequently happens before bone deterioration, malignant bone marrow infiltration can be detected by MRI even before morphologic bone changes are noticeable. Osteolytic disease is frequently associated with hypo- or isointense T1 and hyperintense T2 signals, as well as relatively strong contrast media uptake, which is indicative of the extent of tumor infiltration of the bone marrow. These findings are frequently the result of tumor proliferation in the bone marrow.

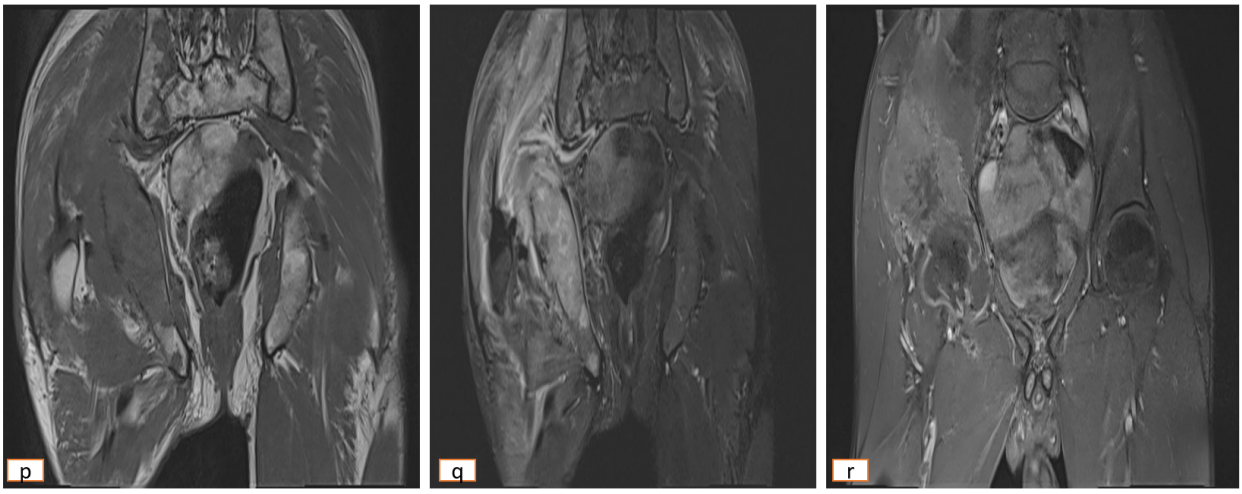

Figure 6: Patient is a 57 yr old male with lung cancer, presented with low backache and hip pain. On MRI of pelvis, a large lobulated expansile p) T1-isointense and T2-hyperintense lesion is noted involving

the right iliac wing, extending to involve the ischium and the right ala of sacrum showing q, r) heterogenous enhancement on post-contrast study. The lesion is also noted to infiltrate the surrounding gluteal muscles. Few similar signal intensity lesions also noted involving head, neck and proximal shaft of bilateral femur, showing enhancement on post-contrast study. Few rim-enhancing collections also noted involving the gluteal muscles. Features favouring the diagnosis of a bone metastasis.

Case 7- Tenosynovial Giant-cell tumor: Tenosynovial giant cell tumor (TGCT) is a fibrohistiocytic soft-tissue tumor that affects anatomical structures such as bursae, tendon sheaths, and joints that are covered in a synovial membrane. Additionally, extra-synovial sites like subcutaneous and intramuscular lesions may be impacted [43]. Pain, edema, stiffness, and restricted function are typical symptoms that lower one's quality of life [44].

TGCT can be categorized based on its growth pattern and site (intra- and extra-articular) [45]. The terms "giant cell tumor of the tendon sheath" and "pigmented villonodular synovitis" were replaced with "localized-type" (L-TGCT) and "diffuse-type" (D-TGCT) in the 2013 World Health Organization classification of soft tissue and bone tumors [43].

MRI is the modality of choice to diagnose D-TGCT. For the purpose of identifying hemosiderin linked to tumor bleeding, a gradient-echo sequence might be useful. Intravenous gadolinium contrast is useful for post-synovectomy follow-up and tumor detection. Because of its heterogeneous histological composition and the range of growth patterns (intra-and/or extra-articular), TGCT can present with variable MRI appearances [45]. Unusual synovial thickening (> 5 mm), usually characterized as "frond-like" with villous or nodular morphology, is one of the findings of D-TGCT [45]. The associated reactive joint effusion is often engulfed by this synovial proliferation, leading to multiloculated thick-walled trapped cystic masses. This is particularly evident in Baker's cysts and the subgastrocnemius synovial recesses, respectively [43]

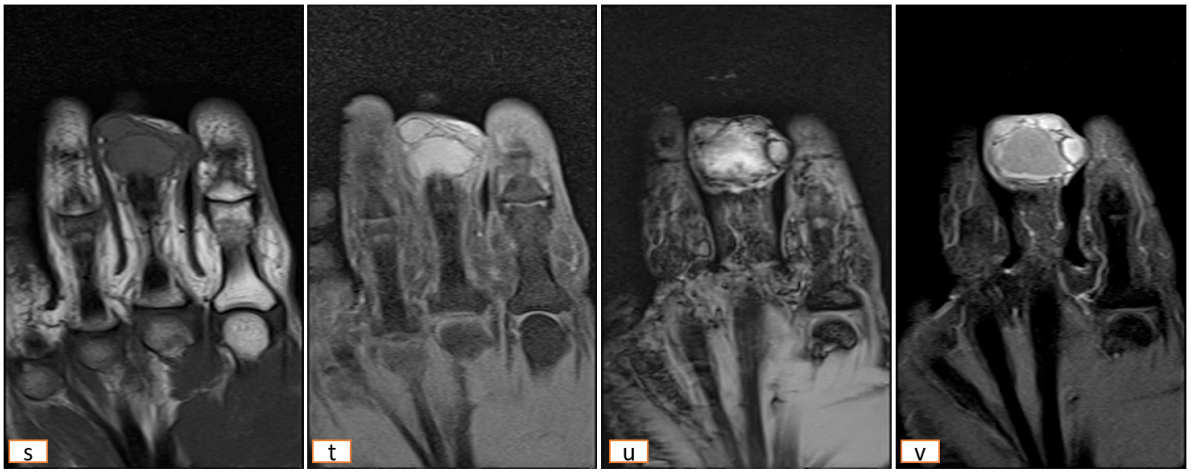

Figure 7: A s) T1-isointense and t) T2FS- hyperintense lesion is noted on the volar aspect of 3rd digit, adjacent to the middle phalanx, closely abutting the flexor tendon. The lesion shows blooming foci on u) SWI/GRE sequence and shows v) heterogenous enhancement on post-contrast study. However, no hyperintensity is noted involving the substance of the flexor tendon and no underlying bone erosion also seen. Features are consistent with tenosynovial giant cell tumor.

Case 8- Schwannoma: Schwannomas are benign neurogenic tumors that arise from nerve sheath cells. Of all benign soft tissue neoplasms, they are 5% more common in the second to fifth decade of life [46-49]. Intramuscular schwannomas are rare tumors. Intramural schwannomas manifest as a slow-growing soft tissue mass in patients, who may or may not experience accompanying neurological symptoms.

The preoperative diagnosis of intramuscular schwannoma has been found to benefit from MR imaging [47–50]. The split-fat sign, a low signal margin, the fascicular sign, and a hyperintense rim are MR imaging findings that corroborate the diagnosis of intramuscular schwannoma. The nerve's entry and exit signs are a reliable and frequently observed MR imaging characteristic of schwannomas.

The entry and exit sign forms on T2-weighted MR images due to a hyperintense signal located longitudinally to a fusiform mass.

The distinction between neurofibromas and schwannomas can be made with the aid of MR imaging. Whereas neurofibromas are not encapsulated, Schwannomas are typically located

in an eccentric position within the nerve. When separating benign nerve tumors from malignant peripheral nerve sheath tumors (MPNSTs), magnetic resonance imaging (MRI) is the preferred imaging technique.

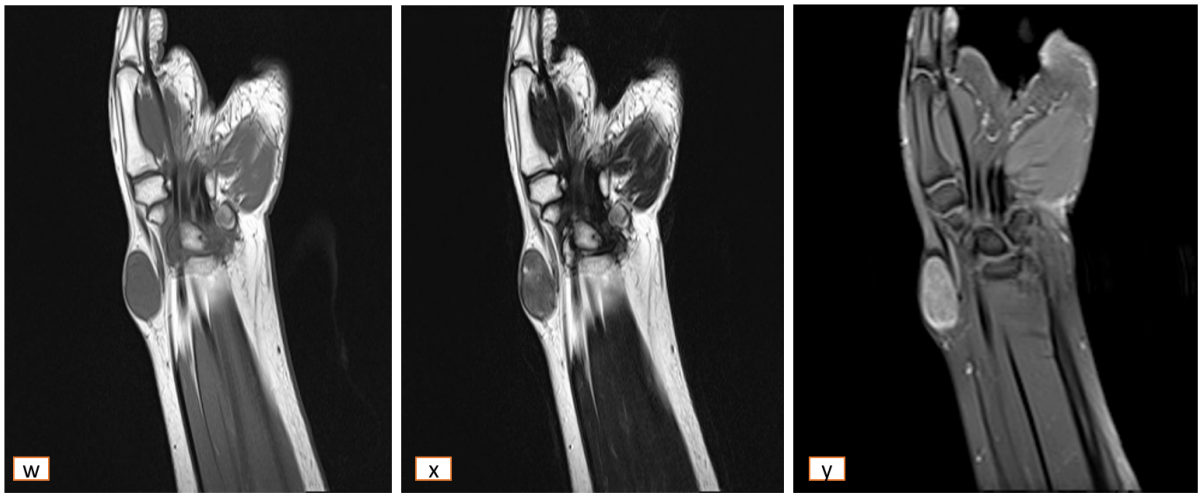

Figure 8: Fusiform shaped w) T1/T2 isointense mass lesion with few internal cystic changes is noted in the radial side of the wrist, located in the subcutaneous plane, showing y) mild contrast enhancement on post contrast study. The mass lesion has tapered ends with nerves seen leading into and out of the mass possibly cutaneous branch of radial nerve. Possibly schwannoma.

Conclusion

A good knowledge of the characteristic MRI findings of benign and malignant osseous conditions and their role in staging, therapeutic planning and follow-up in the setting of malignancy is essential for optimal patient care.

Bone tumors and tumor-like lesions are frequently encountered by radiologists. Although radiographs are the primary screening technique, magnetic resonance imaging (MRI) can help narrow the differential or make a specific diagnosis when a lesion is indeterminate or shows signs of aggressiveness.

MRI can extend the diagnostic evaluation by demonstrating several tissue components. Even when a specific diagnosis cannot be made, the differential diagnosis can be narrowed. MRI is superior to the other imaging modalities in detecting bone marrow lesions and tumoral tissue (faint lytic/sclerotic bone lesions can be difficult to visualize using only radiographs). Contrast-enhanced MRI can reveal the most vascularized parts of the tumor and MRI guidance makes it possible to avoid biopsing necrotic areas. MRI is very helpful in local staging and surgical planning by assessing the degree of intramedullary extension and invasion of the adjacent physeal plates, joints, muscle compartments and neurovascular bundles.

Acknowledgements: The authors would like to thank the Department of Medicine, Silchar Medical College and Hospital for their clinical contribution.

Competing Interests: The authors affirm that no personal or financial relationships that may have inappropriately influenced them in writing this article.

Authors' Contributions: A.N., B.P., and T.K. contributed significantly and equally to this work.

Ethical Considerations: Informed consent was obtained from all individual participants involved in the study.

Data Availability: The authors confirm that the data supporting the findings of this research are available within the article.

Disclaimer

The views and opinions expressed in this article are those of the authors and do not necessarily reflect the official policy or position of any affiliated agency of the authors.

References

1. Madewell JE, Ragsdale BD, Sweet DE. Radiologic and pathologic analysis of solitary bone lesions. I. Internal margins. Radiol Clin North Am 1981; 19:715–748.
2. Ragsdale BD, Madewell JE, Sweet DE. Radiologic and pathologic analysis of solitary bone lesions. II. Periosteal reactions. Radiol Clin North Am 1981; 19:749–783.
3. Sweet DE, Madewell JE, Ragsdale BD. Radiologic and pathologic analysis of solitary bone lesions. III. Matrix patterns. Radiol Clin North Am 1981; 19:785–814.
4. Priolo F, Cerase A. The current role of radiography in the assessment of skeletal tumors and tumor-like lesions. Eur J Radiol 1998; 27(suppl 1):S77–S85.

5. Kricun ME. Radiographic evaluation of solitary bone lesions. Orthop Clin North Am 1983; 14:39–64.
6. Brown KT, Kattapuram SV, Rosenthal DI. Computed tomography analysis of bone tumors: patters of cortical destruction and soft tissue extension. Skeletal Radiol 1986; 15:448–451.
7. Seeger LL, Dungan DH, Eckardt JJ, Bassett LW, Gold RH. Nonspecific findings on MR imaging: the importance of correlative studies and clinical information. Clin Orthop Relat Res 1991; 270:306–312.
8. Hayes CW, Conway WF, Sundaram M. Misleading aggressive MR imaging appearance of some benign musculoskeletal lesions. RadioGraphics 1992; 12:1119–1136.
9. Ma LD, Frassica FJ, Scott WW, Fishman EK, Zerhouni EA. Differentiation of benign and malignant musculoskeletal tumors: potential pitfalls with MR imaging. Radio- Graphics 1995; 15:349–366.
10. Choi JH, Ro JY. The 2020 WHO Classification of Tumors of Bone: An Updated Review. Adv Anat Pathol 2021; 28(3):119–138.
11. Kadhim M, Thacker M, Kadhim A, Holmes L Jr. Treatment of unicameral bone cyst: systematic review and meta-analysis. J Child Orthop 2014;8(2):171–191.
12. Campanacci M, Capanna R, Picci P. Unicameral and aneurysmal bone cysts. Clin Orthop Relat Res 1986 ;(204):25–36.
13. D'Amato RD, Memeo A, Fusini F, Panuccio E, Peretti G. Treatment of simple bone cyst with bone marrow concentrate and equine-derived demineralized bone matrix injection versus methylprednisolone acetate injections: A retrospective comparative study. Acta Orthop Traumatol Turc 2020; 54(1):49–58.
14. Cho HS, Oh JH, Kim HS, Kang HG, Lee SH. Unicameral bone cysts: a comparison of injection of steroid and grafting with autologous bone marrow. J Bone Joint Surg Br 2007; 89(2):222–226.
15. Bezirgan U, Karaca MO, Merter A, et al. Steroid Injection and Biomarker Levels in the Treatment of Unicameral Bone Cysts: Can we Estimate the Result? Indian J Orthop 2021; 55(4):886–891.
16. Kadhim M, Sethi S, Thacker MM. Unicameral Bone Cysts in the Humerus: Treatment Outcomes. J Pediatr Orthop 2016; 36(4):392–399.
17. Heimdahl A. An unusual case of 'simple bone cyst' of the mandible. Int J Oral Surg 1978; 7:32-/5.
18. Cottalorda J, Bourelle S. Modern concepts of primary aneurysmal bone cyst. Arch Orthop Trauma Surg. 2007 Feb; 127(2):105-14.
19. Jee WH, Choi KH, Choe BY, Park JM, Shinn KS (1996) Fibrous dysplasia: MR imaging characteristics with radiopathologic correlation. AJR Am J Roentgenol 167(6):1523–1527
20. Atalar MH, Salk I, Savas R, Uysal IO, Egilmez H (2015) CT and MR imaging in a large series of patients with craniofacial fibrous dysplasia. Pol J Radiol 80:232–240
21. Murphey MD, Senchak LT, Mambalam PK, Logie CI, Klassen-Fischer MK, Kransdorf MJ. From the radiologic pathology archives: ewing sarcoma family of tumors: radiologicpathologic correlation. Radiographics 2013; 33(3): 803–831
22. El Weshi A, Allam A, Ajarim D, et al. Extraskeletal Ewing's sarcoma family of tumours in adults: analysis of 57 patients from a single institution. Clin Oncol (R Coll Radiol) 2010;22(5):374–381
23. Kim SW, Shin H. Primary intradural extraosseous Ewing's sarcoma. J Korean Neurosurg Soc 2009;45(3):179–181
24. Downing JR, Head DR, Parham DM, et al. Detection of the (11;22) (q24;q12) translocation of Ewing's sarcoma and peripheral neuroectodermal tumor by reverse transcription polymerase chain reaction. Am J Pathol 1993;143(5):1294–1300
25. Nagaraj P, Srinivas CH, Rao R, Manohar S. Extra skeletal soft tissue Ewing's sarcoma with variant translocation of chromosome t(4; 22)(q35; ql2)-A case report. J Orthop Case Rep 2013;3(4):12–15
26. Christie DRH, Bilous AM, Carr PJA. Diagnostic difficulties in extraosseous Ewing's sarcoma: a proposal for diagnostic criteria. Australas Radiol 1997;41(1):22–28
27. Bhat AP, Schuchardt PA, Bhat R, Davis RM, Singh S. Metastatic appendiceal cancer treated with Yttrium 90 radioembolization and systemic chemotherapy: A case report. World J Radiol 2019;11(9):116–125
28. O'Keeffe F, Lorigan JG, Wallace S. Radiological features of extraskeletal Ewing sarcoma. Br J Radiol 1990;63(750):456–460
29. Klein MJ, Siegal GP. Osteosarcoma: anatomic and histologic variants. Am J Clin Pathol 2006; 125(4): 555–581.
30. Damron TA, Ward WG, Stewart A. Osteosarcoma, chondrosarcoma, and Ewing's sarcoma: National Cancer Data Base report. Clin Orthop Relat Res 2007; 459:40–47.
31. Mirabello L, Troisi RJ, Savage SA. Osteosarcoma incidence and survival rates from 1973 to 2004: data from the Surveillance, Epidemiology, and End Results Program. Cancer 2009; 115(7):1531–1543.
32. Murphey MD, Robbin MR, McRae GA, Flemming DJ, Temple HT, Kransdorf MJ. The many faces of osteosarcoma. RadioGraphics 1997; 17(5): 1205–1231.

33. Zambo I, Veselý K. WHO classification of tumours of soft tissue and bone 2013: the main changes compared to the 3rd edition [in Czech]. Cesk Patol 2014; 50(2):64–70.
34. Moore DD, Luu HH. Osteosarcoma. Cancer Treat Res 2014; 162:65–92.
35. Ritter J, Bielack SS. Osteosarcoma. Ann Oncol 2010; 21(suppl 7):vii320–vii325.
36. Zeitoun R, Shokry AM, Ahmed Khaleel S, Mogahed SM. Osteosarcoma subtypes: magnetic resonance and quantitative diffusion weighted imaging criteria. J Egypt Natl Canc Inst 2018; 30(1):39–44.
37. Bielack S, Carrle D, Casali PG; ESMO Guidelines Working Group. Osteosarcoma: ESMO clinical recommendations for diagnosis, treatment and follow-up. Ann Oncol 2009;20(suppl 4):137–139.
38. Weiss A, Khoury JD, Hoffer FA, et al. Telangiectatic osteosarcoma: the St. Jude Children's Research Hospital's experience. Cancer 2007; 109(8):1627–1637.
39. Onikul E, Fletcher BD, Parham DM, Chen G. Accuracy of MR imaging for estimating intraosseous extent of osteosarcoma. AJR Am J Roentgenol 1996; 167(5):1211–1215.
40. O'Flanagan SJ, Stack JP, McGee HM, Dervan P, Hurson B. Imaging of intramedullary tumour spread in osteosarcoma: a comparison of techniques. J Bone Joint Surg Br 1991;73(6):998–1001.
41. Gillespy T 3rd, Manfrini M, Ruggieri P, Spanier SS, Pettersson H, Springfield DS. Staging of intraosseous extent of osteosarcoma: correlation of preoperative CT and MR imaging with pathologic macroslides. Radiology 1988; 167(3):765–767.
42. Han G, Wang Y, Bi WZ, et al. Magnetic resonance imaging is appropriate for determining the osteotomy plane for appendicular osteosarcoma after neoadjuvant chemotherapy. Med Oncol 2012; 29(2):1347–1353.
43. de St. Aubain Somerhausen N, Van de Rijn M (2020) Tenosynovial giant cell tumour. In: WCoTEB (ed) 5th World Health Organization Classification of Tumours of Soft Tissue and Bone. IARC Press, Lyon
44. Gelhorn HL, Tong S, McQuarrie K et al. Patient-reported symptoms of tenosynovial giant cell tumors. Clin Ther 2016; 38(4):778–793
45. Murphey MD, Rhee JH, Lewis RB, Fanburg-Smith JC, Flemming DJ, Walker EA. Pigmented villonodular synovitis: radiologic-pathologic correlation. Radiographics 2008; 28(5): 1493–1518
46. Kransdorf MJ. Benign soft-tissue tumors in a large referral population: distribution of specific diagnoses by age, sex, and location. AJR Am J Roentgenol 1995; 164:395-402.
47. Enzinger FM, Weiss SW. Benign tumors of peripheral nerves. In: Soft tissue tumors, eds. St Louis, MO: Mosby, 1995: 821-88.
48. Murphey MD, Smith WS, Smith SE, Kransdorf MJ, Temple HT. From the archives of the AFIP. Imaging of musculoskeletal neurogenic tumors: radiologic-pathologic correlation. Radiographics 1999; 19:1253-80.
49. Shimose S, Sugita T, Kubo T, et al. Major-nerve schwannomas versus intramuscular schwannomas. Acta Radiol 2007; 48:672-7.
50. Cerofolini E, Landi A, DeSantis G, et al. MR of benign peripheral nerve sheath tumors. J Comput Assist Tomogr 1991; 15:593-7.